J Appl Electrochem (2009) 39:779–784
DOI 10.1007/s10800-008-9720-2

ORIGINAL PAPER

Synergistic inhibition between the gemini surfactant and bromide ion for steel corrosion in sulphuric acid

**Zhen-Yu Wu · Zheng Fang · Ling-Guang Qiu ·
Yun Wu · Zong-Qun Li · Tao Xu ·
Wei Wang · Xia Jiang**

Received: 11 June 2008 / Accepted: 6 November 2008 / Published online: 28 November 2008

Abstract The inhibitive synergistic effect between a cationic gemini surfactant, 1,3-propane-bis(dimethyl dodecylammonium bromide) (12-3-12), and bromide ion for the corrosion inhibition of cold rolled steel in 0.5 mol L^{-1} H_2SO_4 was investigated by weight loss, potentiodynamic polarization method and electrochemical impedance spectroscopy (EIS). The inhibition system composed by 12-3-12 and bromide ion is efficient. The adsorption mechanism of the 12-3-12 and bromide ion on steel in acidic medium is discussed on the basis of experimental data and an adsorption model is proposed. Adsorption of inhibitor system on the mild steel surface in acidic medium obeys Langmuir's adsorption isotherm. In addition, potentiodynamic polarization studies show that the system acts as a mixed-type inhibitor. Electrochemical impedance spectroscopy also suggests the formation of a protective layer on the steel surface by the adsorption of surfactant molecules and bromide ions.

Keywords Gemini surfactant · Synergistic effect · Adsorption · Potentiodynamic polarization · Electrochemical impedance spectroscopy (EIS)

1 Introduction

Surfactants have been widely used as corrosion inhibitors for some metals and alloys in cleaning, pickling and petroleum industries processes [1–14]. The inhibiting action of surfactant compounds on the corrosion of carbon steel in aqueous media is usually related to their adsorption on the metal surface. Adsorption results in an effective blocking of the active sites of metal dissolution and/or hydrogen evolution, thus diminishing the overall corrosion rate. As a new generation of surfactant, gemini surfactants have attracted great interest in recent years [15–18]. This kind of surfactant is constituted by two hydrophilic groups and two hydrophobic groups in the molecule, separated by a spacer. Compared with conventional single-chained surfactants, corresponding gemini surfactants are more efficient to form micelles, show lower critical micelle concentration (CMC), better solubilization and greater efficiency in lowering the surface tension of water. As a novel kind of promising inhibitor for corrosion of steel in corrosive medium, cationic gemini surfactants have been demonstrated to be highly efficient for steel corrosion inhibition in acidic medium [19–26]. However, the great expense of gemini surfactants retards their application in various industrial processes.

The application of the synergistic effect between a corrosion inhibitor and another chemical substance is an effective means to improve the performance of inhibitors and reduce the cost for corrosion protection. Halide ions are effective additives for quaternary ammonium surfactants in corrosion inhibition systems for steel in acidic media [26–30]. In this work, the inhibitive synergistic effect between a cationic gemini surfactant, 1,3-propane-bis(dimethyldodecylammonium bromide) (12-3-12) and bromide ion for the corrosion inhibition of cold rolled steel

---

Z.-Y. Wu · Z. Fang
School of Chemistry and Chemical Engineering, Central South University, Changsha 410083, China

Z.-Y. Wu · L.-G. Qiu (✉) · Y. Wu · Z.-Q. Li · T. Xu ·
W. Wang · X. Jiang
School of Chemistry and Chemical Engineering, Key Laboratory of Environment-Friendly Polymer Materials of Anhui Province, Anhui University, Hefei 230039, China
e-mail: lgqiu@ahu.edu.cn

in 0.5 mol L^{-1} H_2SO_4 was investigated by weight loss, the potentiodynamic polarization method and electrochemical impedance spectroscopy. The results show that this novel inhibition system is efficient for corrosion inhibition of steel in sulphuric acid medium. Based on the Langmuir adsorption model, some adsorption parameters are estimated, and the adsorption mechanism is discussed. Potentiodynamic polarization studies show that the inhibition system is mixed-type. EIS results are in good agreement with those obtained by the potentiodynamic polarization and weight loss data.

2 Experimental

Potassium bromide and sulphuric acid were purchased from Shanghai Chemical Reagent Co. Ltd. (Shanghai, China). Double distilled water was used for preparing test solutions for all measurements. Cold rolled steel sample with composition C $\leq$0.1%, Mn $\leq$0.50%, P $\leq$0.035%, S $\leq$0.025% and the remainder Fe was obtained from Cold Rolled Mill Plant of Baosteel (Shanghai, China). Gemini surfactant 12-3-12 was prepared as described previously and the CMC of the surfactant was determined to be 9.69×10^{-4} mol L^{-1}, according to the break points in plots of the specific conductance versus concentration of gemini surfactants in 25 °C [23].

The weight loss experiment was carried out as reported previously [22–26] and the corrosion rate of steel (r_{corr}) was calculated by the relation

$$r_{corr} = (w_1 - w_2)/St \tag{1}$$

where w_1 and w_2 are the weight of the specimen before and after corrosion, respectively, S the area of the specimen, and t the corrosion time.

Potentiodynamic polarization and EIS measurements were carried out in a conventional three-electrode cell on a CHI604C Electrochemical Work Station (Shanghai Chenhua, China) with a platinum counter electrode (CE), a saturated calomel electrode (SCE) as the reference electrode, and a working electrode made of cold rolled steel rods of 0.85 cm diameter. The rod specimen was embedded in epoxy resin mould and only its cross-section was allowed to contact the electrolyte solutions. The electrode was polished on a series of emery papers down to 5,000 grit (991A, MATADOR®, Germany), washed thoroughly with distilled water and then acetone under the ultrasonic, and finally dried in the air. Subsequently, the electrode was immersed in test solution for 0.5 h and then allowed to reach a stable open-circuit potential (OCP). The potentiodynamic current potential curves were recorded by automatically changing the electrode potential from −250 to +250 mV vs. corrosion potential (E_{corr}) at a scanning rate of 0.5 mV s^{-1}. The frequency range for EIS used was from 100 kHz to 0.05 Hz at corrosion potential (E_{corr}). The amplitude of the applied sinusoidal signal was 5 mV, resistances and capacitances were determined by fitting the EIS data with an equivalent circuit. All potentials were measured with respect to the SCE. All electrochemical experiments were carried out in aerated solutions at a temperature of (30 ± 0.02) °C.

3 Results and discussion

3.1 Weight loss method

3.1.1 Corrosion inhibition of steel in 0.5 mol L^{-1} H_2SO_4 by 12-3-12 at 30 °C

Corrosion rates of cold rolled steel in the presence of gemini surfactant 12-3-12 in various concentrations in 0.5 mol L^{-1} sulphuric acid were determined at 30 °C. It was found that the corrosion rate decreased remarkably from 10.08 to 1.16 g m^{-2} h^{-1} with increasing 12-3-12 concentration from 0 to 1.0×10^{-3} mol L^{-1}. Above this concentration, however, increasing surfactant concentration did not affect corrosion rate significantly. This result is similar to our previous study on corrosion inhibition of carbon steel in 1 mol L^{-1} hydrochloric acid by the gemini surfactants alkanediyl-α,ω-bis(dimethyl dodecylammonium bromide) [23].

3.1.2 Effect of KBr on inhibition of 12-3-12 for steel corrosion in 0.5 mol L^{-1} H_2SO_4

To clarify synergistic effects between the gemini surfactant 12-3-12 and bromide ion for corrosion inhibition of steel, corrosion rates of cold rolled steel in 0.5 mol L^{-1} sulphuric acid in the presence of 12-3-12 (1×10^{-6} mol L^{-1}, at which the inhibition efficiency ($E\%$) was approximately 50%) and KBr in different concentrations (0–0.5 mol L^{-1}) were determined at different temperatures as shown in Fig. 1. The corrosion rates of steel in 0.5 mol L^{-1} H_2SO_4 in the presence of 1×10^{-6} mol L^{-1} of 12-3-12 were found to be 1.6–5.7 g m^{-2} h^{-1} depending on the corrosion temperature from 25 to 40 °C. However, the addition of KBr to the above system resulted in a significant decrease in corrosion rates until the KBr concentration was higher than 0.3 mol L^{-1}. It is clear that Br^- anions play a dominate role in the corrosion inhibition of steel in the presence of the cationic surfactant. The inherent reason is that the steel surface has positive charge and it is difficult for the positively charged cationic surfactant molecules to approach this positively charged steel surface. However, the specific adsorption of Br^- on the positively charged

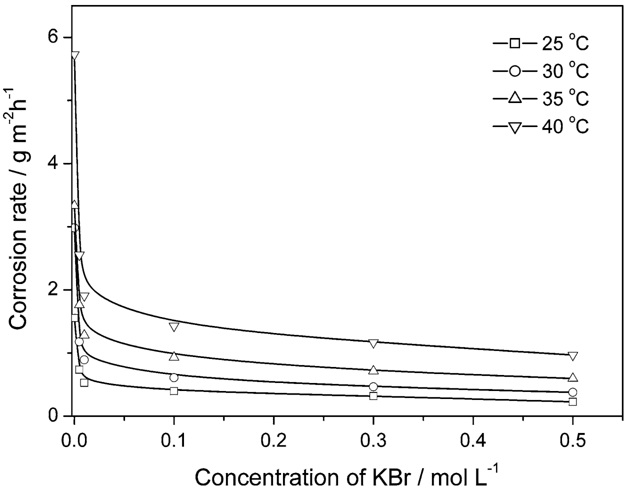

Fig. 1 Variation of the corrosion rate with KBr concentration in the presence of 12-3-12 (1×10^{-6} mol L^{-1}) at different temperatures: (*open square*) 25 °C; (*open circle*) 30 °C; (*up-pointing traingle*) 35 °C; (*down-pointing traingle*) 40 °C

steel surface by means of electrostatic attraction results in a negatively charged surface layer. Thus cationic surfactant molecules can be adsorbed readily on the steel surface by electrostatic interaction between Br$^-$ layer and the cationic surfactant, thus leading to a significant decrease in corrosion rate.

3.1.3 Adsorption of 12-3-12 and 12-3-12/KBr on steel surface in 0.5 mol L^{-1} H$_2$SO$_4$

In our previous studies it was found that the adsorption of gemini surfactant conformed to the Langmuir adsorption model [22–26] According to this model

$$\frac{c}{\theta} = \frac{1}{K} + c \tag{2}$$

where c is the inhibitor concentration, θ the surface coverage whose value may be evaluated from Eq. 3, and K the modified adsorption equilibrium constant as defined in Eq. 4:

$$\theta = \frac{W_0 - W}{W_0 - W_m} \tag{3}$$

$$K = \frac{1}{c_{\mathrm{solvent}}} \exp\left(\frac{-\Delta G_{\mathrm{ads}}}{\mathrm{RT}}\right) \tag{4}$$

where W_0 and W are the values of the weight loss without and with addition of the surfactant, respectively, W_{m} the smallest weight loss, c_{solvent} the molar concentration of the solvent, which in the case of water is 55.5 mol L^{-1}. R is the universal gas constant, T the absolute temperature and ΔG_{ads} the change in Gibbs free energy of adsorption.

After calculating the surface coverage for the 12-3-12 and 12-3-12/KBr systems under different conditions, the linear regression between c/θ and c, values of K, and Gibbs free energy change (ΔG_{ads}) for adsorption of 12-3-12 or 12-3-12/Br$^-$ on steel in 0.5 mol L^{-1} sulphuric acid were calculated. The results are summarized in Table 1. Both the correlation coefficients and the slope of straight line $c/\theta \sim c$ approached 1, suggesting that the adsorption of 12-3-12 molecules and Br$^-$ conforms to Langmuir's adsorption model as described above. Also, both values of ΔG_{ads} for 12-3-12 and 12-3-12/Br$^-$ are negative, suggesting the spontaneity of the adsorption; the ΔG_{ads} values for 12-3-12 (around -42 kJ mol^{-1}) were more negative than those for 12-3-12/KBr (around -26 to -30 kJ mol^{-1} at 25–40 °C), which indicates high adsorption ability and strong tendency of 12-3-12 molecules to adsorb on steel in comparison with 12-3-12 in the presence of bromide ions.

According to another form of the Langmuir model derived for corrosion inhibition, one obtains [31–33]:

$$\frac{1}{r_{\mathrm{corr}}} = K'' + K'c \tag{5}$$

where K'' is a constant that is equal to the inverse of the corrosion rate without inhibitor, and K' another constant. A plot of $1/r_{\mathrm{corr}}$ versus concentration of the inhibitor should yield a linear relationship if the Langmuir model is obeyed. For conventional single-chained surfactants, one transition (near CMC) was found in the plot of $1/r_{\mathrm{corr}}$ versus surfactant concentration, which was attributed to the transition from monolayer to multilayer of the surfactant molecules [31].

Table 1 Adsorption parameters of 12-3-12 and 12-3-12/KBr system on the steel surface in 0.5 mol L^{-1} sulphuric acid at various temperatures

Inhibitor	T (°C)	R	Slope	$1/K$	K	ΔG_{ads} (kJ mol^{-1})
12-3-12	30	1.0000	0.9807	3.37×10^{-6}	2.97×10^{5}	−41.88
12-3-12/KBr[a]	25	0.9999	1.0082	1.54×10^{-3}	6.49×10^{2}	−26.01
	30	1.0000	1.0086	9.48×10^{-4}	1.05×10^{3}	−27.67
	35	1.0000	1.0074	9.08×10^{-4}	1.10×10^{3}	−28.23
	40	1.0000	1.0032	6.65×10^{-4}	1.50×10^{3}	−29.50

[a] c(12-3-12) = 1×10^{-6} mol L^{-1}

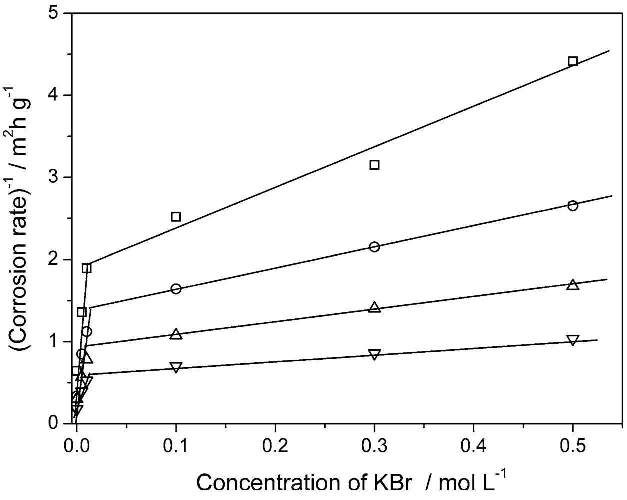

Fig. 2 Variation of $1/r_{corr}$ with KBr concentration for 12-3-12/KBr system at different temperatures: (*open square*) 25 °C; (*open circle*) 30 °C; (*up-pointing traingle*) 35 °C; (*down-pointing traingle*) 40 °C

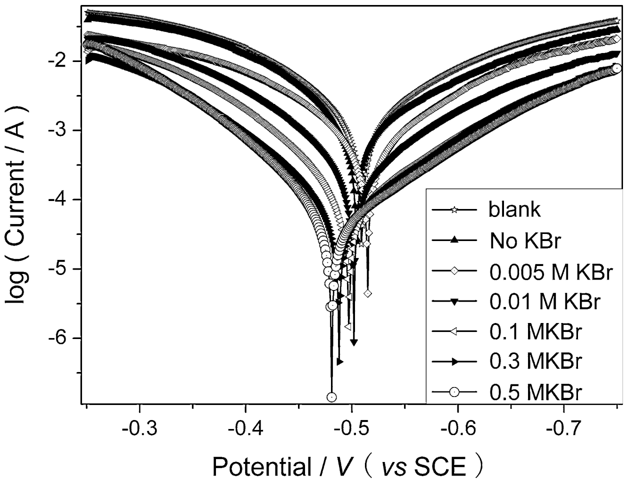

Fig. 3 Potentiodynamic polarization curves for gemini surfactant 12-3-12 and 12-3-12/KBr system on the steel surface in 0.5 mol L^{-1} sulphuric acid at 30 °C

However, two transition points (near CMC and c*) were found in plots of $1/r_{corr}$ versus concentration of the gemini surfactants in our previous results [22–26]. This was explained by the difference in molecular structure between gemini surfactant and traditional single-chained surfactant [22–26].

Similarly to our previous studies, two transition points (near CMC and c*) were found in plots of $1/r_{corr}$ versus 12-3-12 concentration at 30 °C. However, only one transition was found for 12-3-12/KBr (see Fig. 2), suggesting that the adsorption mechanism of bromide ion on the steel surface in acidic medium in the presence of 12-3-12 is similar to the conventional surfactant. This may be attributed to the relatively low concentration of 12-3-12 (1×10^{-6} mol L^{-1}). In such a low concentration of 12-3-12 only part of the surface is covered by molecules of the gemini surfactant 12-3-12, and the rest is occupied by bromide ions.

3.2 Electrochemical methods

3.2.1 *Polarization studies*

Both anodic and cathodic polarization curves for cold rolled steel in 0.5 mol L^{-1} H_2SO_4 in the presence of 12-3-12 (1×10^{-6} mol L^{-1}, at which the inhibition efficiency ($E\%$) was approximately 50%) and KBr in different concentrations (0–0.5 mol L^{-1}) are shown in Fig. 3. The inhibition efficiency ($E\%$) is defined as:

$$E\% = \left(\frac{I_{corr} - I_{corr(inh)}}{I_{corr}}\right) \times 100 \tag{6}$$

where I_{corr} and $I_{corr(inh)}$ are the corrosion current density values without and with inhibitor, respectively, as determined by extrapolation of Tafel lines to the corrosion potential.

The presence of inhibitor causes a marked decrease in corrosion rate, i.e. shifts the anodic curves to more positive potentials and the cathodic curves to more negative potentials. This may be ascribed to adsorption of inhibitor over the surface. The values of corrosion current densities (I_{corr}), corrosion potential (E_{corr}), potentiodynamic polarization resistance (Rp) and the inhibition efficiency (IE%) as functions of KBr concentration in the presence of 12-3-12 of 1×10^{-6} mol L^{-1}, were calculated from the curves of Fig. 3 and the results are listed in Table 2.

The corrosion current clearly decreases while IE% increases with increase in KBr concentration. Furthermore, the presence of 12-3-12 and KBr does not remarkably shift the corrosion potential, while the anodic and cathodic Tafel slopes change with increasing KBr concentration. Therefore, the synergistic inhibition system of 12-3-12 and KBr can be regarded as a mixed-type inhibitor in 0.5 mol L^{-1} H_2SO_4.

3.2.2 *EIS studies*

The impedance data for steel in 0.5 M H_2SO_4 in the absence and presence of 12-3-12/KBr are shown in Figs. 4, 5, and 6. All plots have a depressed semicircular in the complex impedance plane with the center under the real axis. This typical behavior for solid metal electrodes shows frequency dispersion of the impedance data and can be attributed to roughness and other inhomogeneities of the surface. In these cases the parallel net charge transfer resistance-double layer capacitance ($R_{ct} - C_{dl}$) is usually accepted as a poor approximation, especially for systems where an efficient inhibitor is present. When a non-ideal frequency response is

Table 2 Potentiodynamic polarization parameters and the values of elements of equivalent circuit to fit the impedance spectra for gemini surfactant 12-3-12/KBr system for corrosion inhibition of steel in 0.5 mol L^{-1} sulphuric acid at 30 °C

C_{inh}	E_{corr} (V vs. SCE)	Rp (ohm)	I_{corr} (μA/cm^{-2})	E (%)	CPE (Y_0/μΩ^{-1} cm^{-2}S^n)	n (0–1)	R_{ct} (Ω cm^{-2})	E (%)
Blank	−0.509	12.22	2871.00	/	367.95	0.8936	31.63	/
No KBr[a]	−0.504	23.52	1319.00	54.06	277.84	0.8984	77.15	58.93
0.005 M[a]	−0.515	35.42	851.50	70.34	129.13	0.8749	154.50	79.53
0.01 M[a]	−0.502	80.77	326.50	88.63	109.70	0.8555	347.30	90.89
0.1 M[a]	−0.497	182.40	127.10	95.56	92. 26	0.8394	446.40	92.91
0.3 M[a]	−0.488	271.50	79.64	97.22	68.51	0.8301	662.80	95.23
0. 5 M[a]	−0.497	372.00	31.16	98.90	42.26	0.8358	786.90	95.98

[a] c(12-3-12) = 1 × 10^{-6} mol L^{-1}

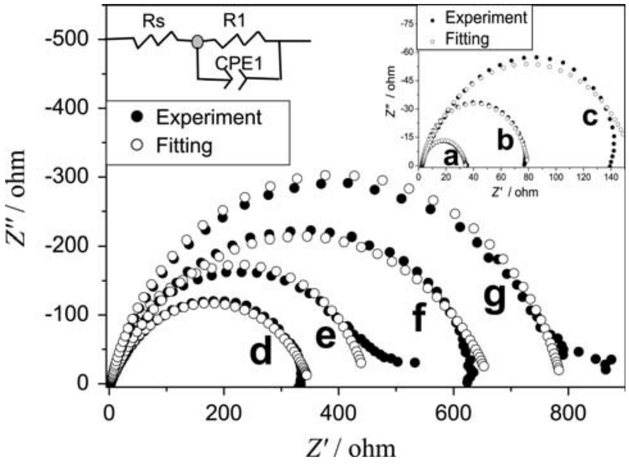

Fig. 4 Equivalent circuit for synergistic inhibition in mol L^{-1} H_2SO4 and Nyquist plots of experiment and fitting system 12-3-12/KBr system with concentration of KBr at 30 °C. (a) Blank, (b) no KBr, (c) 0.005 M KBr, (d) 0.01 M KBr, (e) 0.1 M KBr, (f) 0.3 M KBr, (g) 0.5 M KBr

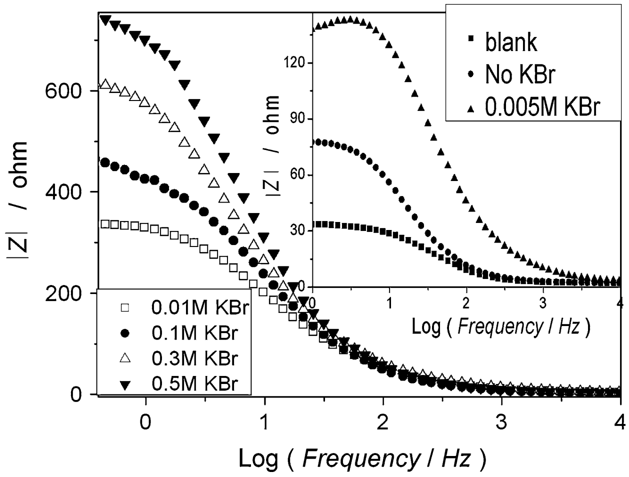

Fig. 5 |Z| plots of 12-3-12/ KBr system with concentration of NaCl at 30 °C

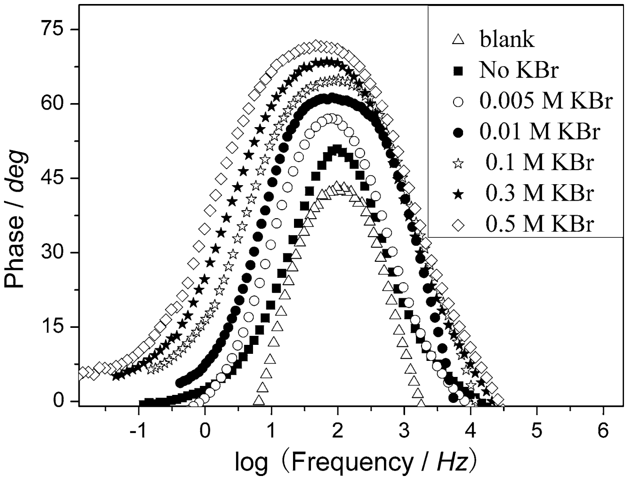

Fig. 6 Phase angle plots of 12-3-12/ KBr system with concentration of KBr at 30 °C

present, it is commonly accepted to employ distributed circuit elements in the equivalent circuit. The most widely used is the constant phase element (CPE), which has a non-integer power dependence on the frequency. CPE is often used in a model in place of a capacitor to compensate for non-homogeneity in the system. The impedance of a CPE is described by the expression:

$$Y_{CPE} = Y_0(j\omega)^n \qquad (7)$$

where Y_0 is the modulus, ω the angular frequency (in rad s^{-1}). $j^2 = -1$ is the imaginary number and n represents phase shift and can be used as a measure of the surface inhomogeneity [1–4]. For $n = 0$, Y_{CPE} represents a resistance with $R = Y_0$, for $n = 1$, a capacitance with $C = Y_0^{-1}$, for $n = 0.5$, a Warburg element, and for $n = -1$ an inductance with $L = Y_0$.

The equivalent circuit in Fig. 4 was used to analyze and fit impedance spectra in the present work. In the circuit, R_s is the resistance of solution between the iron electrode and the reference electrode, and R_1 (corresponding to R_{ct}) is the charge-transfer resistance corresponding to the corrosion reaction at the metal substrate/solution interface. The double-layer usually behaves as a constant phase element (CPE) rather than a pure capacitor. In the equivalent circuit, CPE is substituted for a pure capacitor so that the impedance spectra is fitted better. The inhibition efficiency $E\%$ was calculated by the following expression:

$$E\% = \frac{R_{\mathrm{ct}} - R_{\mathrm{ct0}}}{R_{\mathrm{ct}}} \tag{8}$$

where R_{ct0} and R_{ct} are values of the charge transfer resistance (Ω m^2) observed in the absence and presence of inhibitor, respectively.

Based on the model mentioned above, the experimental data for blank and 12-3-12/KBr system in 0.5 mol L^{-1} H_2SO_4 were fitted and the results are shown in Fig. 5 and Table 2. The capacitance Y_0 (corresponding to C_{dl}) decreases with increase in R_{ct}, indicating surface adsorption of surfactant film. The decrease in C_{dl}, which may result from a decrease in local dielectric and/or increase in thickness of the electrical double layer, implies that surfactant molecules function by adsorption on the steel surface. In addition, Z, R_{ct} and phase angle increase with increase in KBr concentration (see Figs. 4, 5, and 6), suggesting that inhibition efficiency increases with KBr concentration. The analysis of the parameters associated with the capacitive loop reveals that the capacity of the double layer decreases with increase in inhibitor concentration. This means that as gemini surfactant adsorbs, the Helmholtz layer is influenced because water molecules and other ions are displaced. The decrease in the capacity with increasing surfactant concentrations may be attributed to the formation of a protective layer at the electrode surface.

4 Conclusion

The synergistic effect between gemini surfactant and bromide ions was studied using weight loss, potentiodynamic polarization and electrochemical impedance spectroscopy (EIS) methods. 12-3-12/KBr synergistic inhibitor system was found to be an excellent and cost-efficient inhibitor for steel corrosion in sulphuric acid. The values of ΔG_{ads} for 12-3-12 and 12-3-12/Br$^-$ systems in acidic medium suggest the spontaneity of the adsorption. The adsorption mechanism of bromide ion in the presence of 12-3-12 was different from that of 12-3-12. In addition, potentiodynamic polarization studies show that the 12-3-12/Br$^-$ system is a mixed-type inhibitor.

Acknowledgements We are grateful for the financial support from the Key Project of Natural Science Foundation from Education Bureau of Anhui Province (kj2007A078), and Selected Financial Support Research Project from Education Bureau of Anhui Province, China.

References

1. Atia AA, Saleh MM (2003) J Appl Electrochem 33:171
2. Mohammed AA (2006) J Appl Electrochem 36:215
3. Gopi D, Manimozhi KS, Govindaraju M, Manisankar P, Rajeswari S (2007) J Appl Electrochem 37:439
4. Ma H-Y, Chen S-H, Yin B-S, Zhao S-Y, Liu X-Q (2003) Corros Sci 45:867
5. Li X-H, Deng S-D, Mu G-N, Fu H, Yang F-Z (2008) Corros Sci 50:420
6. Chebabe D, Ait Chikh Z, Dermaj A, Rhattas K, Jazouli T, Hajjaji N, El Mdari F, Srhiri A (2004) Corros Sci 46:2701
7. Deyab MA (2007) Corros Sci 49:2315
8. Soror TY, El-Ziady MA (2002) Mater Chem Phys 77:697
9. Abd El Rehim SS, Hassan HH, Amin MA (2003) Mater Chem Phys 78:337
10. Osman MM, El-Ghazawy RA, Al-Sabagh AM (2003) Mater Chem Phys 80:55
11. Migahed MA (2005) Mater Chem Phys 93:48
12. Saleh MM (2006) Mater Chem Phys 98:83
13. Rafiquee MZA, Saxena N, Khan S, Quraishi MA (2008) Mater Chem Phys 107:528
14. Tavakoli H, Shahrabi T, Hosseini MG (2008) Mater Chem Phys 109:281
15. Esumi K, Ueno M (1997) Structure-performance relationships in surfactants, surface science series, vol 70. Marcel Dekker, New York
16. Alargova RG, Kochijashky II, Sierra ML, Kwetkat K, Zana R (2001) J Colloid Interface Sci 235:119
17. Menger FM, Keiper JS (2000) Angew Chem Int Ed Engl 39:1906
18. Oda R, Panizza P, Lequeux F (1997) Prog Colloid Polym Sci 105:276
19. El Achouri M, Kertit S, Gouttaya HM, Nciri B, Bensouda Y, Perez L, Infante MR, Elkacemi K (2001) Prog Org Coat 43:267
20. El Achouri M, Infante MR, Izquierdo F, Kertit S, Gouttaya HM, Nciri B (2001) Corros Sci 43:19
21. Yao S-Z, Jiang X-H, Zhou L-M, Lv Y-J, Hu X-Q (2007) Mater Chem Phys 104:301
22. Qiu L-G, Xie A-J, Shen Y-H (2005) Corros Sci 47:273
23. Qiu L-G, Xie A-J, Shen Y-H (2005) Appl Surf Sci 246:1
24. Qiu L-G, Xie A-J, Shen Y-H (2005) Mater Chem Phys 91:269
25. Qiu L-G, Wu Y (2007) In: EL Bettini (ed) Progress in corrosion research, Nova Science Publishers, Inc., New York, pp 159–185
26. Qiu L-G, Wu Y, Wang Y-M, Jiang X (2008) Corros Sci 50:576
27. Tang L-B, Li X-M, Mu G-N, Liu G-H, Li L, Liu H-C, Si Y-S (2006) J Mater Sci 41:3063
28. Trabanelli G (1991) Inhib Corros 47:410
29. Sanyal B (1981) Prog Org Coat 9:165
30. Schweinsberg DP, Ashworth V (1988) Corros Sci 28:539
31. Free ML (2002) Corros Sci 44:2865
32. Free ML (2004) Corros Sci 46:3101
33. Free ML, Wang WL (2004) Corros Sci 46:2601